# Uncertainty quantification of network availability for networks of optical ground stations

Iñigo del Portillo, Marc Sanchez-Net, Bruce G. Cameron, Edward F. Crawley

Iñigo del Portillo, Marc Sanchez-Net, Bruce G. Cameron, Edward F. Crawley, "Uncertainty quantification of network availability for networks of optical ground stations," Proc. SPIE 10096, Free-Space Laser Communication and Atmospheric Propagation XXIX, 100961B (24 February 2017); doi: 10.1117/12.2251819

SPIE.

Event: SPIE LASE, 2017, San Francisco, California, United States

# Uncertainty quantification of network availability for networks of optical ground stations

Iñigo del Portillo†, Marc Sanchez-Net†, Bruce G. Cameron†, and Edward F. Crawley†

†Massachusetts Institute of Technology, 77 Massachusetts Avenue, Cambridge, USA 02139

## ABSTRACT

This paper analyzes differences in the availability of networks of optical ground stations computed using different methods and datasets, and quantifies the uncertainty of the results. For that purpose, we first review existing methods proposed in the literature, and then existing cloud coverage datasets, and we compare the results obtained using different methods and datasets for several scenarios. Finally, we propose a new probabilistic global cloud coverage model that aggregates values from existing datasets and quantifies the uncertainty in measuring cloud probability, and present a method to compute the availability of a network of multiple optical ground stations, along with the corresponding uncertainty.

**Keywords:** Uncertainty analysis; Satellite system availability; Optical ground station network; Space-to-ground optical communications.

## 1. INTRODUCTION

Free space optical communications is envisioned as the next milestone in space communications, due to the higher data-rates achievable (an increase of 10 to 100 times compared to current RF technology), and its lower size, mass, and power. The main drawback of this technology is the decrease in network availability due to link outages caused by cloud coverage, for which site diversity has been proposed as a mitigation technique.

In the last few years, several studies have been conducted to determine the optimal location of the optical ground stations (OGSs), both for networks that serve geostationary satellites,[1–3] as well as for those that serve satellites in LEO orbit.[4] In addition, these studies can be broadly classified into two groups: those that use high-frequency historical cloud coverage data to estimate the availability of the network,[1,2,5,6] and those that develop probabilistic models based on long-term averages.[3,4,7,8] However, no analyses have been conducted to quantify the uncertainty of the results when a) the inputs of the models come from different datasets, and b) the network availability is computed using different methods.

As a motivational example, let us consider a network with 5 ground stations that serves a geostationary satellite over the European-African region, as shown in Figure 1a, and analyze the average network availability for every month in the period 2004-2007. The network availability is computed using two high frequency historical datasets (EUMETSAT-hf and ISCCP-hf) which register the presence or absence of clouds at regular time intervals (1 and 3 hours respectively), and the probabilistic model described by Sanchez-Net[8] fed with cloud-probability estimates obtained from monthly cloud fraction datasets (AIRS, ISSCP, MODIS, PATMOSX, and POLDER). Figure 1b shows the average monthly link outage probabilities (LOP) for the years 2004-2008. Differences of over 500% are found when using ISCCP (the dataset that estimates the highest LOP) and MODIS-CE (the dataset that estimates the lowest LOP). Figure 1c shows the year-average for the LOP: between the maximum value of 0.0143 (ISCCP), and the minimum value of 0.00123 (MODIS-CE), there is more than one order of magnitude of difference.

Further author information: (Send correspondence to Iñigo del Portillo. portillo@mit.edu)

Free-Space Laser Communication and Atmospheric Propagation XXIX, edited by Hamid Hemmati, Don M. Boroson,
Proc. of SPIE Vol. 10096, 100961B · © 2017 SPIE · CCC code: 0277-786X/17/$18 · doi: 10.1117/12.2251819

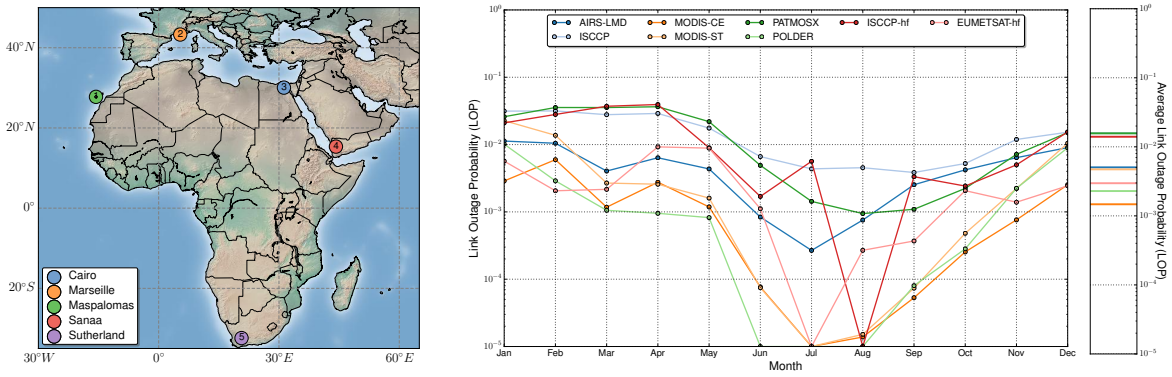


(a) Ground station location for the motivational example.

(b) Average monthly link outage probability (years 2004-2008).

(c)

Figure 1: Global model for cloud probability and associated uncertainty.

In view of the results for this example, it can be difficult to conclude whether the availability of this network is 99 % or 99.9 %. Furthermore, the results of this analysis are only valid for the period 2004-2008, and one could question their validity if other periods of time are considered. To answer these questions, this paper analyzes the differences in network availabilities when using different methods and datasets, and quantifies the uncertainty of the results. For this, we first review the uncertainty associated with the methods proposed in the literature and with the existing cloud coverage datasets . Next, we propose a new global cloud coverage model that accounts for uncertainty, and a method to compute the network availability and the uncertainty associated with this measure. Finally, we present network availability results produced using this method.

## 2. UNCERTAINTY ANALYSIS

As shown in our previous motivational example, different results are obtained when using different datasets and methods to evaluate network availability. In that sense, there is a reasonable doubt over how well the results represent the network availability that would actually be obtained, had the real network been operational. This *reasonable doubt* is referred to as uncertainty, defined by *Guide to the expression of uncertainty in measurement* (GUM)[9] as "a parameter, associated with the result of a measurement, that characterizes the dispersion of the values that could reasonably be attributed to the *measurand*". Particularly, the term *measurement* in the definition refers to the algorithm or procedure used to estimate the value of a given quantity, which is the value of the *measurand*.

The GUM includes a list of different sources of uncertainty in the estimation of the *measurand*, of which the following cases are most relevant for the study of optical network availability (ONA):

- **Approximations and assumptions incorporated in the measurement method**: Some methods used to compute the network availability assume that the weather conditions at different ground stations located at different locations are uncorrelated, when in reality this is not the case. The uncertainty associated with approximations and assumptions within the measurement methods is quantified in Section 2.1.1.
- **Variations in repeated observations of the measurand under identical conditions**: When computing the network availability, some algorithms generate a synthetic sequence of cloud coverage for each location. These sequences are generated by drawing random numbers from a given probability distribution, and since randomness is inherent to the algorithms, the ONA estimations derived present a degree of uncertainty. The uncertainty associated with such approximation and assumptions is quantified in Section 2.1.2.

- **Inexact values of parameters obtained from external sources and used in the estimation algorithms**: A vast majority of the methods employed to assess the network availability use as inputs estimates of the cloud-probabilities at the locations of the OGSs. These estimates present a degree of uncertainty arising from the instruments and the algorithms used to derive them. The uncertainty due to inexact values of the cloud probability datasets is analyzed in Section 2.2

## 2.1 UNCERTAINTY IN AVAILABILITY MODELS

Methods to evaluate the LOP of a network of optical ground stations can be classified into simulation models and analytical models. Simulation models compute the network availability from historical or synthetically-generated binary sequences of cloud observations, where values denote the presence or absence of clouds over a ground station at a particular time. Analytical models estimate network availability using probabilistic models that use cloud probabilities at each given location as inputs. The main advantage of analytical models is that they offer a computationally efficient way of evaluating millions of architectures, which makes them apt for performing trade-off studies, what-if analyses, and network optimization studies. However, analytical models normally incur in additional sources of error as simplifying assumptions are necessary.

In this Section, we quantify the uncertainties associated with both simulation and analytical methods proposed in the literature.

### 2.1.1 Analytical models

One of the simplest models used to assess the availability of a network of ground stations is the uncorrelated model, wherein the weather conditions in the different locations are assumed to be statistically uncorrelated. The optical network availability (ONA) of a network of N ground stations is given by ONA $= 1 -$ LOP. If "availability" is defined as having *at least one* OGS not covered by clouds, the LOP is computed as

$$\mathrm{LOP} = p_1 \cdot p_2 \cdots p_N, \tag{1}$$

where $p_i$ is the cloud probability of the i-th ground station. If the uncertainty associated with the cloud probability of the i-th ground station is denoted by $u_i$, the uncertainty on the LOP is

$$\left(\frac{u_{\mathrm{LOP}}}{\mathrm{LOP}}\right)^2 = \sum_{i=1}^{N}\left(\frac{d\mathrm{LOP}}{dp_i}u_i\right)^2 \quad \rightarrow \quad u_{\mathrm{LOP}} = \sqrt{\sum_{i=1}^{N}\left[u_i \cdot \prod_{j=1,j\neq i}^{N} p_j\right]^2}. \tag{2}$$

To better understand how the LOP uncertainty depends on the number of ground stations, a simplifying assumption is to consider that all the ground stations have the same cloud probabilities ($p_i = p_j = p,\ \forall i,j$) and uncertainties ($u_i = u_j = u,\ \forall i,j$). Under this equal-probability and equal-uncertainty assumption, Eq. 1 simplifies to $u_{\mathrm{LOP}} = \sqrt{N}\left(p^{(N-1)} \cdot u\right)$, which grows as $\sqrt{N}$ when the number of ground stations increases. Figure 2b shows that the LOP relative uncertainty ($u_{\mathrm{LOP}}/\mathrm{LOP}$) also grows as $\sqrt{N}$, and only depends on the values of the single sites' relative uncertainty ($u/p$). Figure 2a shows the uncertainty associated with the LOP in this scenario. It can be observed that 6 OGSs are required to achieve a 99.9% availability (with 95% confidence) when the single site cloud probability is 0.25 (blue line) and the relative uncertainty is 30%, while only 5 were necessary when uncertainty was not taken into account. If the single site cloud probability is increased to 0.5 (orange line) and the relative uncertainty remains at 30%, 12 OGSs are required to achieve a 99.9% availability with 95% confidence, while only 10 are necessary when uncertainty is not taken into account.

In some cases availability is defined as having at least M out of the N ground stations having clear skies simultaneously (see Gharanjik[10]). In these scenarios, given that the the number of available ground stations is characterized by a Poisson-binomial distribution,[11] the LOP is computed as:

$$\mathrm{LOP} = \sum_{m=1}^{M-1}\sum_{\mathcal{A}\in F_m}\prod_{i\in\mathcal{A}}(1-p_i)\prod_{j\in\mathcal{A}^c}p_j \tag{3}$$

where $\mathcal{F}_m$ is the set of all subsets of m integers that can be selected from $\{1, 2, 3, ..., N\}$. For example, assuming N = 5 ground stations and M = 1, then $F_k = \{\{1\}, \{2\}, \{3\}, \{4\}, \{5\}\}$ and LOP $= p_1p_2p_3p_4(1-p_5) + ... + (1-p_1)p_2p_3p_4p_5$. Furthermore, Eq. 3 can be further simplified if all the ground stations are assumed to have the same cloud probability ($p_i = p_j = p \; \forall i, j$) and uncertainty. In this particular case, the LOP and the uncertainty associated with it are:

$$\text{LOP} = \sum_{m=0}^{M-1} \binom{N}{m} (1-p)^m p^{(N-m)} \tag{4}$$

$$u_{\text{LOP}} = \sqrt{\left[\sum_{m=0}^{M-1} \binom{N}{m} \left[m(1-p)^{m-1}p^{(N-m)} + (N-m)(1-p)^m p^{(N-m-1)}\right]\right]^2 u^2}$$

$$= \sqrt{\left[\sum_{m=0}^{M-1} \binom{N}{m} \left[(1-p)^{m-1}p^{(N-m-1)}(m - N(1-p))\right]\right]^2 u^2} \tag{5}$$

Figure 2c shows the results of the multiple-site availability for the LOP and associated uncertainty. This graph is similar to Fig. 1 in [Fuchs and Moll][1] , but includes the uncertainty boundaries for single site relative uncertainties of $u/p = 10\%$. Finally, Figure 2d shows the relative uncertainty for multiple-site availability versus the number of ground stations. It can be observed that there is a dependence between the relative uncertainty and M: the larger the number of ground stations that must present clear skies to establish a successful communication, the lower the relative uncertainty.

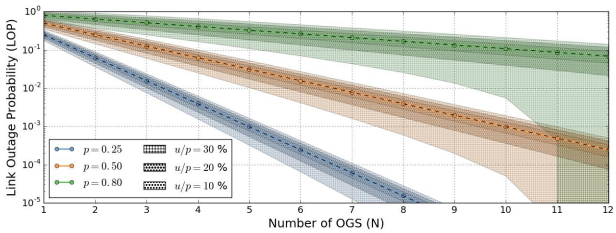


(a) Link outage probability for at least one-site availability for different cloud probabilities ($p$) (uniform across sites) and relative standard uncertainties ($u/p$) versus number of ground stations in the network.

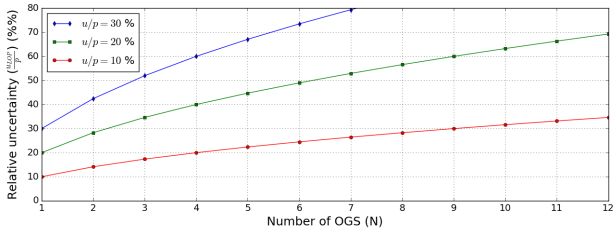


(b) Relative uncertainty versus number of ground stations.

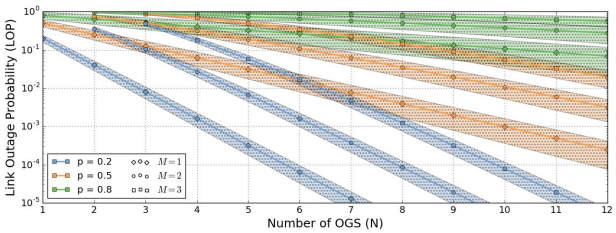


(c) Link outage probability for multiple station availability (M = 1, 2, 3) for different single-site cloud probabilities $p$ and relative uncertainty ($u/p = 10\%$) versus different number of stations in the network.

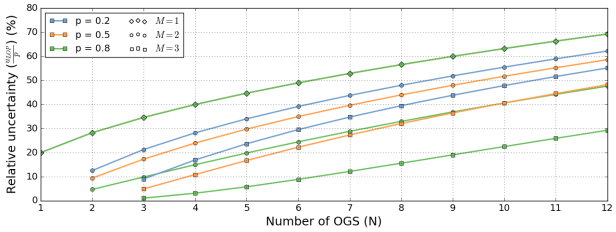


(d) Relative uncertainty for multiple station availability (M = 1, 2, 3) versus number of ground stations

Figure 2: Link outage probabilities and uncertainty for uncorrelated ground stations networks. The shaded region in figures (a) and (c) indicates the 95% confidence interval.

### 2.1.2 Simulation models

Both of the analytical models presented in Section 2.1.1 assume that weather conditions across all the ground stations of the network are uncorrelated, which only holds if the distance between ground stations is large

enough (approximately 1,000 km[7]). If that is not the case, the most common approach to compute the network availability is to use simulation models that employ historical or synthetically-generated sequences of clouds observations. In this section, we analyze the uncertainties associated with the Monte Carlo Sampling (MCS) algorithm proposed by Sanchez-Net et. al.[8] to generate synthetic correlated binary sequences. This algorithm uses as inputs the cloud probabilities of each ground station ($p_i$), the correlation matrix between locations ($\rho_{ij}$), and the number of samples to generate for the binary sequences ($M$). The uncertainty in the output of the algorithm is a consequence of the procedure used to generate the binary sequences, which is inherently random.

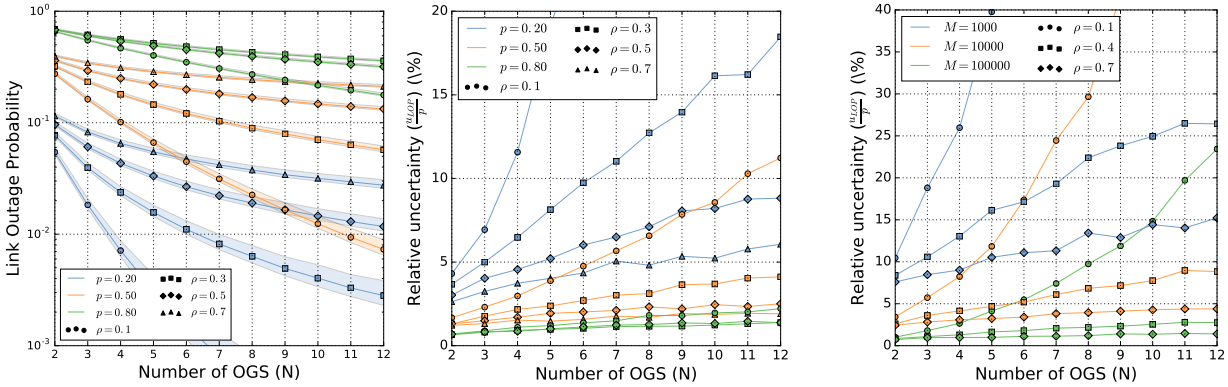


(a) Link outage probability (left) and relative uncertainty(right) vs. cloud probability using the MCS method for different values of $p$ and $\rho$. ($M = 10^4$)

(b) Relative uncertainty vs. number of samples per binary sequence. ($p_i = 0.25$)

Figure 3: Relative uncertainty versus the various inputs of the MCS algorithm proposed by Sanchez-Net.[8]

Figure 3 shows the dependence of the relative uncertainty in the three previously mentioned input parameters of the MCS algorithm. Figure 3a shows that the lower the cloud probability of the ground stations, the larger the relative uncertainty. For a correlation factor across ground stations of $\rho_{ij} = 0.3$ and $M = 10^4$, the relative uncertainty is always below 20 %. In addition, it can be observed that the lower the correlation factor between ground stations, the higher the uncertainty. This suggests that the MCS method is not well suited to analyze networks in which ground stations are uncorrelated, for which the analytical methods presented in Section 2.1.1 are more appropriate. Finally, Figure 3b shows that the relative uncertainty can be reduced if the number of samples per sequence ($M$) is increased. In particular, the relative uncertainty scales with the inverse of $\sqrt{M}$.

Given these observations, the following two recommendations are made:

- When all the correlation coefficients for all of the ground stations in the network are lower than 10 %, use the analytical uncorrelated methods described in Section 2.1.1 to assess the LOP.
- If using the MCS method, use at least $M = 10^5$ samples per binary sequence in order to keep the uncertainty introduced by the approximate MCS method low.
- Extra care must be taken if the ground stations have low cloud probabilities and low correlations, as in this case the uncertainty introduced by the MCS method is maximized. Increasing even further the value of M is a technique to mitigate this effect.

## 2.2 UNCERTAINTY IN CLOUD DATASETS

Satellite-based datasets offer global coverage with high resolutions both in the spatial and temporal domains. This kind of datasets have been used in several previous studies[1–6] to determine the optimal locations for a network of ground stations. Independently of the dataset used to evaluate the network availability, the results will present a certain degree of uncertainty due to a) the uncertainty of the instruments and algorithms used

to detect cloud presence and b) interannual variations in cloud probabilities that are not captured within the time-span of the analysis . The objective of this section is to quantify the uncertainty within these datasets by performing one-to-one comparisons among ten satellite-based datasets (eight of which contain level 3 (L3) data products, while the remaining two contain level 2 data products).

Table 1: Cloud datasets characteristics. AP: Available period, SR: Original dataset spatial resolution, TR: Temporal resolution.

| Name | Inst. Type | AP | SR | TR | Cloud detection procedure | Uncertainty considerations |
|---|---|---|---|---|---|---|
| AIRS-LMD[12] | IR sounder | 2003-2009 | 14km | Month | Uses the AIRS instrument to measure 2378 spectral channels and a posteriori cloud detection algorithm based on spectral coherence of cloud emissivities. | Roughly estimates of the average uncertainty estimate for the cloud amount of 0.05 - 0.15. |
| ATSR-GRAPE[13] | MA imagers (VIS, NIR, IR) | 1997-2009 | 1km | Month | Uses the ORAC algorithm to optimally estimate the presence of clouds using spectral information from the VIS, NIR, and IR bands. | The detection algorithm computes an estimation of the "goodness of fit" for every point. |
| CALIPSO[14] | Lidar | 2007-2008 | 0.48km x 0.34km | Month | The Lidar VIS Attenuated Backscattered profile at 532nm and the Molecular Density are vertically-averaged to a vertical column of 40 levels. | The uncertainty in monthly estimations is high since the number of samples per cell is too low. |
| ISCCP[15] | MS Imagers (VIS, IR) | 1984-2007 | 5km, 30km (sampled) | Month | Emphasizes temporal and spatial over spectral resolution to resolve the diurnal cycle of clouds. Uses multiple satellites to provideglobal coverage. | Estimated uncertainty of 0.05 for monthly means, and estimated accuracy of 0.1. |
| MODIS-CE[16] | MS Imager (VIS,NIR,IR (5 channels)) | 2002-2009 | 1km, 4km (sampled) | Month | Uses a 36 channel instrument that cover the solar and thermal IR spectrum. Provides complete coverage every 2 days. Uses the CERES algorithm for cloud detection. | Reports lower cloud amounts than other datasets. Fails to detect low water clouds and ice clouds of low optical depths. |
| MODIS-ST[17] | MS Imager (VIS,NIR,IR (16 channels)) | 2002-2009 | 1 km | Month | Uses 16 channels that cover the solar and thermal IR spectrum. Provides complete coverage every 2 days. Uses the MOD-35 algorithm for cloud detection. | Validation analysis with CALIOP 1km averaged data shows an agreement of 88% between datasets. |
| PATMOSX [18,19] | MS Imagers (VIS, IR 5 channels) | 1982-2010 | 1km x 5km | Month | Data is based on the AVHRR flown on NOAA and EUMETSAT's polar-orbiting sensors. Uses 6 Bayesian classifiers to determine the presence of clouds. | Depending of the terrain classification, the probability of correct detection varies 0.71 - 0.94. |
| EUMETSAT [20,21] | MS Imager | 2004-2011 | 3km | 1-Hour | SEVIRI measurements of the Meteosat Second Generation satellites are processed by the SAFNWC-MSGv2012 cloud masking algorithm. | L3 probability of detection is higher than 90% and the false alarm ratio is lower than 15%. |
| ISCCP-DX [15] | MS Imagers (VIS, IR) | 1984-2009 | 5km, 30km (sampled) | 3-Hour | Use of threshold classifiers that compare measured radiances and clear sky values for the VIS and IR channels. | Estimated uncertainty of 0.05 for month means, and estimated accuracy of 0.1. |

Table 1 contains a summary of the characteristics of these eleven datasets. Datasets AIRS-LMD, ATSR-GRAPE, CALIPSO-GOCCP, ISCCP, MODIS-CE, MODIS-ST, PATMOS-X, and POLDER all come from the GEWEX Cloud Assessment L3 database,[22] which was an outcome of the GEWEX Radiation Panel.[23] All these datasets have common-format maps of L3 data products (i.e., gridded, monthly statistics) containing different cloud properties such as cloud fraction, cloud top height, cloud thermodynamic phase, etc. In addition, the ISCCP-DX and the EUMETSAT dataset, both containing L2 measures (i.e., measures of geophysical variables at the same resolution and location that the values registered by the instruments' sensors) were included in this analysis. The ISCCP-DX dataset contains 3-hourly observations between 1984-2009 registered by more than 20 satellites, while the EUMETSAT dataset contains hourly observations from the MSG satellites over the African-European region from 2004 to 2011.

Figure 4 shows a comparison of the average monthly cloud probabilities for pairs of datasets using a $1^\circ \times 1^\circ$ spatial grid. The upper left diagonal shows histograms of errors between datasets (i.e., the difference between the values for the cloud probability on each cell of the grid for the two datasets under comparison), and the lower

diagonal shows a table with the bias (mean of the errors), the standard deviation (standard uncertainty), and the number of points compared. The diagonal images show a yearly average of the cloud probabilities for each of the datasets. Errors between all pairs of the datasets derived from the GEWEX study have biases between 0.01 and 0.1, with the standard deviation always below 0.25. Moreover, it can be observed that the POLDER dataset always underestimates the cloud probabilities when compared to the rest of the datasets (which results in lower estimates of the LOP), while the EUMETSAT dataset overestimates it. ATSR-GRAPE is the dataset that shows the highest variance in errors, while ISCCP is the dataset that most-consistently agrees with the rest of datasets and presents the lowest variances.The areas which show the highest errors are the Australian region, the West coast of the US, the Andean region in Chile, Greenland and the Antarctica, which in turn are those that present the lowest cloud probabilities.

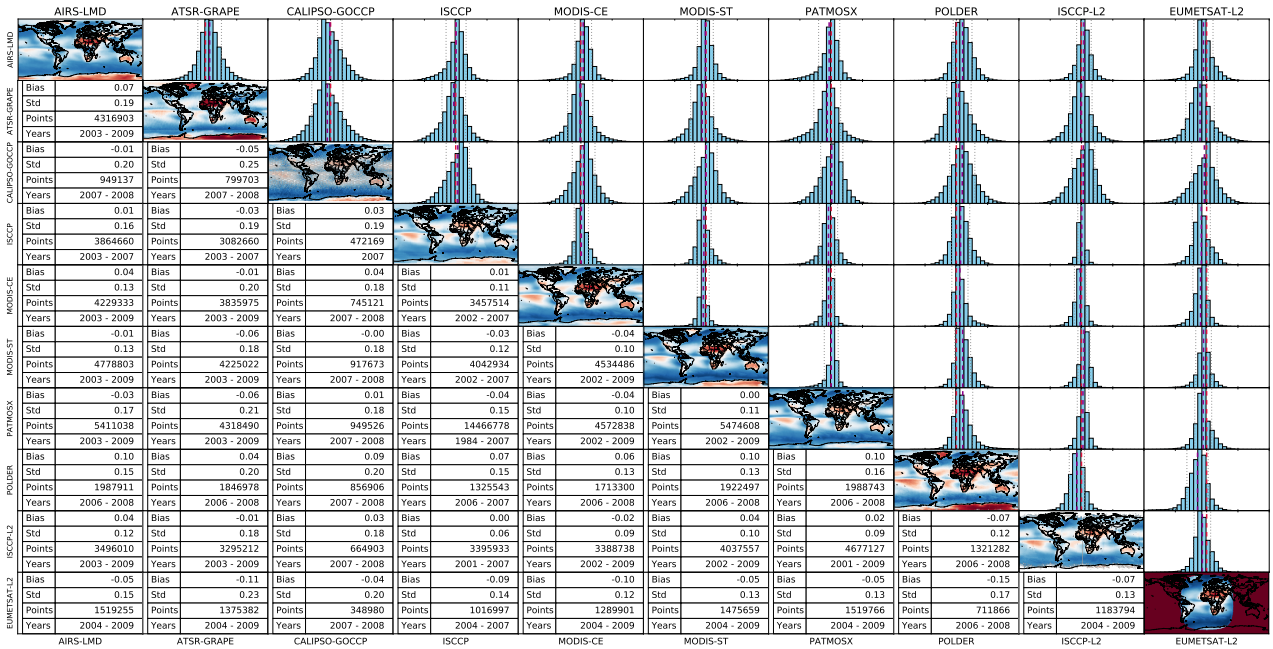


Figure 4: Errors in monthly cloud probabilities for different cloud datasets. The upper diagonal matrix shows the histogram distribution of the errors (the red line represents zero bias, the purple line represents the actual bias, the gray lines indicate the standard deviation), whereas the lower diagonal matrix shows statistical parameters of the error distribution. The errors are computed as dataset in row minus dataset in column.

## 3. INCORPORATING UNCERTAINTY INTO NETWORK AVAILABILITY CALCULATIONS

Section 2.2 analyzed the error distribution between pairs of datasets commonly used to estimate the ONA; in this Section, we explain how to incorporate this information into the network availability computation.

First of all, a model that includes cloud probabilities, together with an estimation of the uncertainties associated with them, is required. For this, we developed a model combining the monthly cloud probability values from the datasets presented in Section 2.2, and characterized the standard uncertainty associated to each latitude-longitude point (with spatial resolution of 1 degree). The monthly cloud probability ($p_{m,ij}$) for each latitude-longitude point per month was computed as the sample mean of all the values for that point in the corresponding month across years,

$$p_{m,ij} = \frac{1}{|\mathcal{Y}|} \sum_{y \in \mathcal{Y}} \frac{1}{|\mathcal{D}_y|} \sum_{d \in \mathcal{D}_y} p_{m,ij}^{(y,d)} \tag{6}$$

where $\mathcal{Y}$ is the set of years for which dataset observations exist, $\mathcal{D}_y$ is the set of datasets that have observations in year $y$, and $p_{m,ij}^{(y,d)}$ is the cloud probability estimate of dataset $d$ in the month $m$ of the year $y$ at the cell $ij$.

The monthly standard uncertainty ($u_{m,ij}$) was computed as the sample standard deviation of all the values for that point in the corresponding month across years. Computed this way, the monthly standard uncertainty takes into account both a) inter-annual variations, and b) different cloud probability estimations obtained using the different datasets.

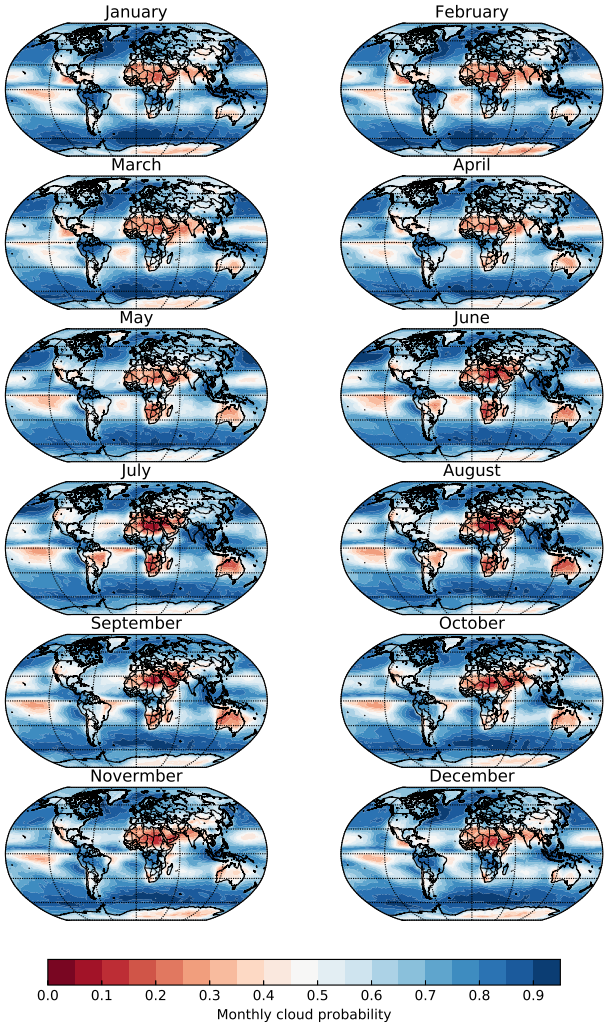


(a) Monthly cloud probability ($p_i$) computed using multiple datasets.

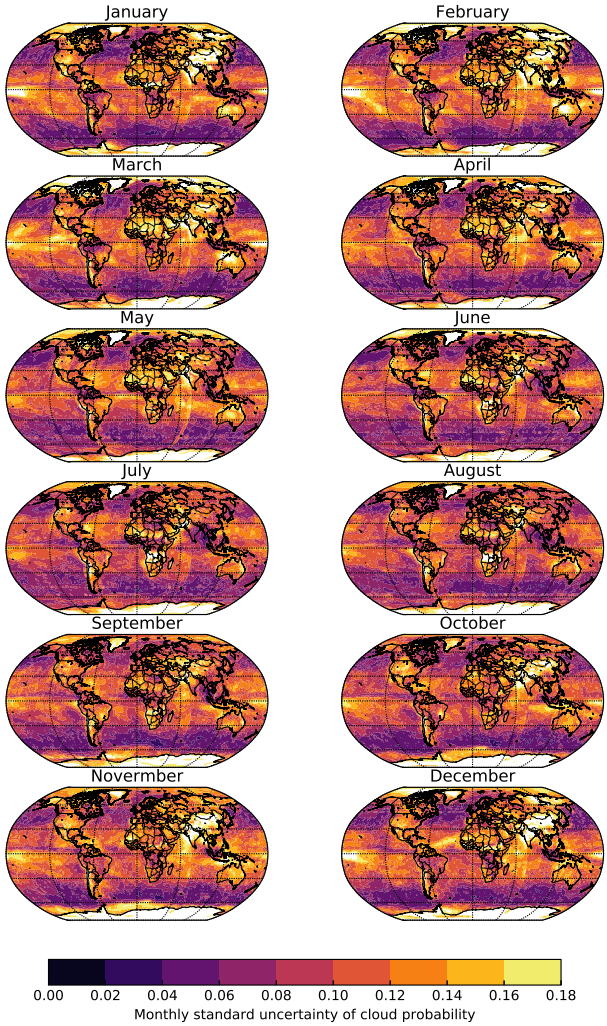


(b) Monthly standard uncertainty ($u_i$) for the cloud probability computed using multiple datasets.

Figure 5: Global model for cloud probability and associated uncertainty.

Figure 5 shows the resulting monthly cloud probability, as well as its associated monthly standard uncertainty. The areas that present the lowest monthly cloud probabilities include the Sahara-region and the South of Africa, the Middle East, Australia and the West coasts of the US and South America. Eastern Asia and India present a seasonal pattern with low monthly cloud probabilities from October to February, and higher cloud probabilities from March to September.

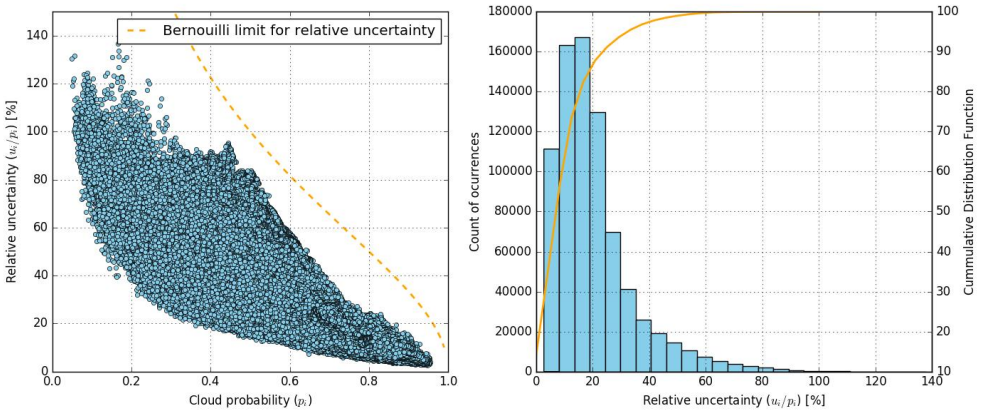


Figure 6: Relative uncertainty vs. cloud probability (left) plus histogram and distribution of relative uncertainty (right).

Figure 6 shows the distribution of the relative uncertainties ($\frac{u_i}{p_i}$) with respect to the cloud probabilities. The dotted orange line indicates the maximum value that the relative uncertainty can take for any given cloud probability. This limit would be reached if the observations that produced the monthly probability have maximal variability and behave as Bernoulli random variables, i.e., the value 1 is present in $p_i$ of the observations and the value 0 in $(1 - p_i)$ of the observations. Furthermore, Figure 6 shows that 90% of the data points present a relative uncertainty lower than 25%, while the relative uncertainty associated with 99% of the cloud probabilities is lower than 60%.

The monthly LOP is computed by the 5 step process described below using the cloud probabilities dataset presented above.

- **Step 1**: For each month of the year and for each OGSs in the network, obtain the cloud probability and the uncertainty associated with it using the dataset presented above.
- **Step 2**: Compute the correlation matrix between ground stations. The correlation coefficients are estimated using the approximation proposed in Garcia et. al.[24]
- **Step 3**: Divide the OGSs into sets of correlated and uncorrelated OGSs. We would consider two OGSs are uncorrelated if the correlation coefficient is inferior to 0.1.
- **Step 4 (a)**: For the uncorrelated sets, evaluate the set monthly LOP and the uncertainty using the analytical methods and equations presented in Section 2.1.1.
- **Step 4 (b)**: For each correlated set, use the method described in Section 2.1.2 to compute the monthly LOP. The uncertainty associated to the LOP ($u_{\text{LOP}}$) is obtained using Monte Carlo Sampling over the input cloud probabilities. Our experiments show that 100 iterations are sufficient to obtain consistent results.
- **Step 5**: Compute the network monthly LOP by multiplying the LOP values obtained in Steps 4a and 4b. The uncertainty associated with the network monthly LOP is obtained using Eq. 1 with $p_i = \text{LOP}$ and $u_i = u_{\text{LOP}}$, where LOP and $u_{\text{LOP}}$ are the values obtained in Steps 4a and 4b.

## 4. RESULTS

Revisiting our motivational example and re-evaluating its LOP with the procedure introduced in the previous section, Figure 7 shows the results of our model together with the results obtained using the datasets introduced in Section 2.2. The shaded area corresponds to the 99% confidence interval, and the right hand plot shows the overall average LOP for the year 2007. Our model shows a high agreement (both in mean and uncertainty)

with the values obtained when using the rest of the datasets to assess the LOP. Furthermore, all of the monthly LOP values obtained using the other datasets fall into the 99 % confidence interval obtained for our uncertainty estimation (assuming a Gaussian distribution for the LOP, the confidence interval is obtained multiplying the standard uncertainty by k = 2.575).

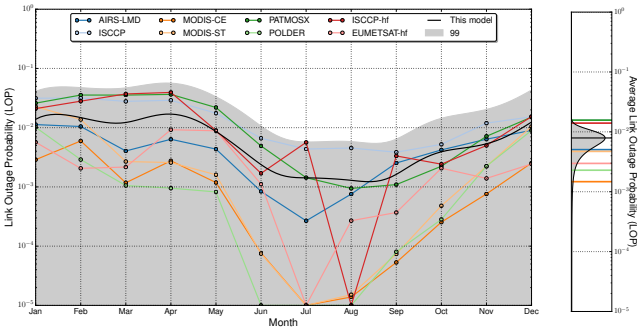


Figure 7: Monthly link outage probability for the example presented in Section 1 computed the model presented in this paper.

Figure 8 shows the results of our model when computing the LOP for 9 different networks compared to the results obtained using other datasets and approximation methods. Again, it can be observed a close agreement between our model and the values obtained using other datasets both for the monthly LOPs and the yearly average LOPs (depicted in the vertical bar to the right hand side). In our experiments our model has correctly computed LOP for networks that present both low and large numbers of OGSs (up to 20 sites). The results obtained agree with the results of Section 2.1: the higher the number of ground station, the larger the relative uncertainty for the LOP. Note that as generally large networks attain lower LOPs, this also implies that the relative uncertainty associated with low LOP values is larger than the uncertainty associated with large LOP values.

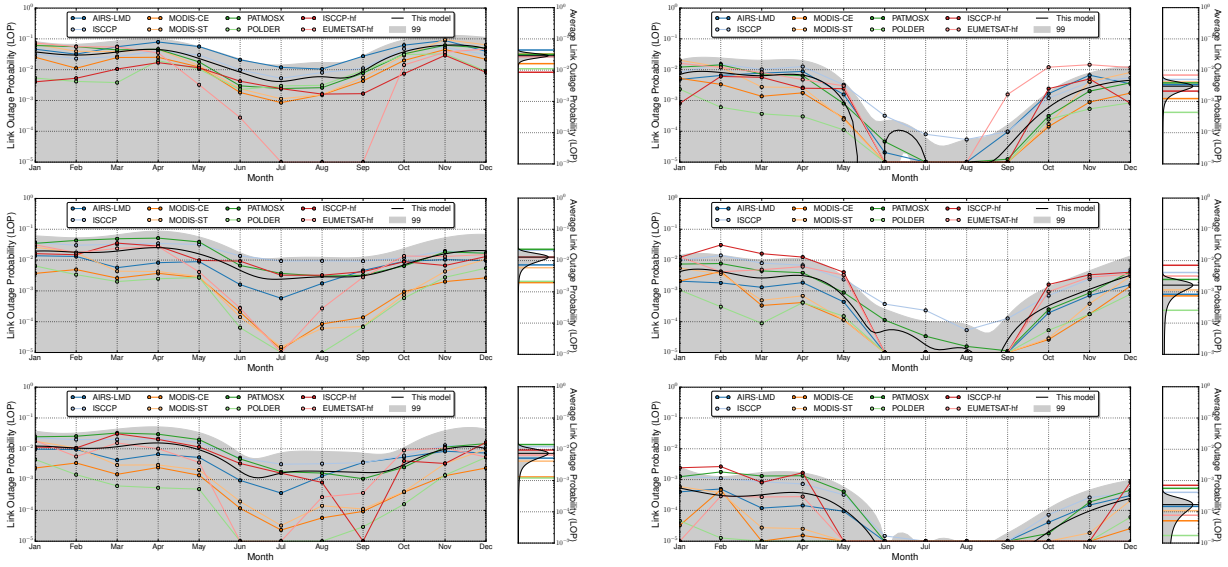


Figure 8: Monthly link outage probabilities for 6 different networks of ground stations.

To compare the results produced by our model to those produced using other datasets, 1,000 architectures were evaluated and the relative error (i.e., $e = \frac{\text{LOP}_d - \text{LOP}_{our}}{\text{LOP}_d}$) was computed for the yearly average LOP. Figure 9a shows the distribution of these errors, and Table 9b shows their bias and standard deviation. We observe that our model's estimations of the yearly average LOP have a low bias when compared to the results obtained using datasets AIRS-LMD and MODIS-ST. However, our model trends to underestimate the yearly average LOP by approximately 25% when compared to the LOPs obtained with datasets ISCCP, PATMOS-X, and EUMETSAT, and to overestimate it when compared to POLDER, MODIS-CE and ISCCP-hf. Both MODIS-CE and POLDER trend to present the lowest LOP estimations, with biases of -126.5% and -285.6 % respectively. The variance of the errors is comprised between 20% and 190%, being ISCCP and PATMOS-X the datasets that present the lowest deviations and POLDER and ISCCP-hf the ones that present the largest ones. This occurs as POLDER and ISCCP-hf trend to produce overly-optimistic LOP estimations for some months (with LOPs close to 0) which results in very large relative errors. Finally, 92.3% of the yearly LOP estimates using the datasets presented in Section 2.2 fell within the 99 % confidence interval computed using the LOP and uncertainty produced by our model. The lower-than-expected value is due to the effects of the results obtained from datasets POLDER and MODIS-CE, which trend to produce much lower yearly average LOP estimates than our model.

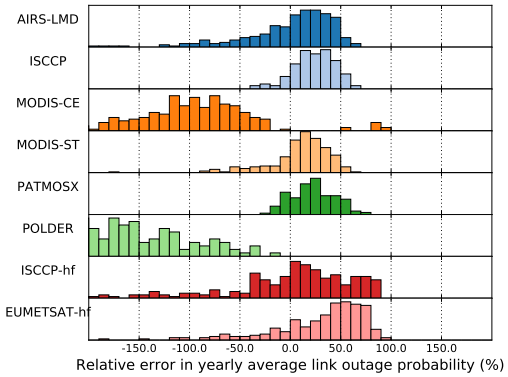


(a) Relative error of the yearly average LOP

| Dataset | Yearly | |
|---|---|---|
| | $E[e_y]$ [%] | $\sigma_y$ [%] |
| AIRS-LMD | -2.5 | 50.3 |
| ISCCP | 23.7 | 20.7 |
| MODIS-CE | -126.5 | 110.3 |
| MODIS-ST | 9.5 | 30.9 |
| PATMOSX | 22.6 | 21.0 |
| POLDER | -285.6 | 186.8 |
| ISCCP-hf | -65.8 | 189.3 |
| EUMETSAT-hf | 24.9 | 61.6 |

(b) Statistical parameters of the relative errors.

Figure 9: Relative errors for the yearly average LOP obtained using our model and other datasets

## 5. CONCLUSIONS

This paper quantifies different sources of uncertainty when evaluating the network availability for a network of optical ground stations. The sources of uncertainty characterized include inexact values of the cloud probability parameters obtained form external datasets, approximations and assumptions incorporated in the estimation algorithms, and variations in repeated observations of the measurand due to randomness in the network availability estimation algorithms. A global model that contains estimates for the cloud probability together with the uncertainty associated to them was developed to serve as the input to a method to estimate both the network link outage probability and the uncertainty associated to this measure. The uncertainty value provides a quantitative assessment of the validity of the LOP results, a feature that previous analyses lacked.

The usefulness of this method was proven through several examples in which the long term monthly and yearly average LOP were computed for different networks. Finally, a comparison of the results produced by this model to those produced by other datasets was performed.

## ACKNOWLEDGMENTS

The GEWEX Cloud Assessment data were obtained from the ClimServ Data Center of IPSL/CNRS. The authors would like to thank the *Fundación Obra Social de La Caixa* for partially funding this project.

## REFERENCES


[1] Fuchs, C. and Moll, F., "Ground station network optimization for space-to-ground optical communication links," *Journal of Optical Communications and Networking* **7**(12), 1148–1159 (2015).

[2] Poulenard, S., Crosnier, M., and Rissons, A., "Ground segment design for broadband geostationary satellite with optical feeder link," *Journal of Optical Communications and Networking* **7**(4), 325–336 (2015).

[3] del Portillo, I., Sanchez, M., Cameron, B., and Crawley, E., "Architecting the ground segment of an optical space communication network," in [*Aerospace Conference, 2016 IEEE*], 1–13, IEEE (2016).

[4] del Portillo, I., Sanchez, M., Cameron, B., and Crawley, E., "Optimal location of optical ground stations to serve leo spacecraft," in [*Aerospace Conference, 2017 IEEE*], 1–16, IEEE (2017).

[5] Wojcik, G. S., Szymczak, H. L., Alliss, R. J., Link, R. P., Craddock, M. E., and Mason, M. L., "Deep-space to ground laser communications in a cloudy world," in [*Optics & Photonics 2005*], 589203–589203, International Society for Optics and Photonics (2005).

[6] Schulz, K., Rush, J., et al., "Optical Link Study Group Final Report," *IOAG-15b, June* (2012).

[7] Perlot, N. and Perdigues-Armengol, J., "Model-oriented availability analysis of optical geo-ground links," in [*SPIE LASE*], 82460P–82460P, International Society for Optics and Photonics (2012).

[8] Net, M. S., nigo del Portillo, I., Crawley, E., and Cameron, B., "Approximation methods for estimating the availability of optical ground networks," *J. Opt. Commun. Netw.* **8**, 800–812 (Oct 2016).

[9] des Poids et Mesures, B. I., électrotechnique internationale, C., and internationale de normalisation, O., [*Guide to the Expression of Uncertainty in Measurement*], International Organization for Standardization (1995).

[10] Gharanjik, A., Liolis, K., Shankar, M. B., and Ottersten, B., "Spatial multiplexing in optical feeder links for high throughput satellites," in [*Signal and Information Processing (GlobalSIP), 2014 IEEE Global Conference on*], 1112–1116, IEEE (2014).

[11] Fernandez, M. and Williams, S., "Closed-form expression for the poisson-binomial probability density function," *IEEE Transactions on Aerospace and Electronic Systems* **46**(2), 803–817 (2010).

[12] Stubenrauch, C., Cros, S., Guignard, A., and Lamquin, N., "A 6-year global cloud climatology from the atmospheric infrared sounder airs and a statistical analysis in synergy with calipso and cloudsat," *Atmospheric Chemistry and Physics* **10**(15), 7197–7214 (2010).

[13] Sayer, A., Poulsen, C., Arnold, C., Campmany, E., Dean, S., Ewen, G., Grainger, R., Lawrence, B. N., Siddans, R., Thomas, G., et al., "Global retrieval of atsr cloud parameters and evaluation (grape): dataset assessment," *Atmospheric Chemistry and Physics* **11**(8), 3913–3936 (2011).

[14] Chepfer, H., Bony, S., Winker, D., Cesana, G., Dufresne, J., Minnis, P., Stubenrauch, C., and Zeng, S., "The gcm-oriented calipso cloud product (calipso-goccp)," *Journal of Geophysical Research: Atmospheres* **115**(D4) (2010).

[15] Rossow, W. B. and Schiffer, R. A., "Advances in understanding clouds from isccp," *Bulletin of the American Meteorological Society* **80**(11), 2261 (1999).

[16] Minnis, P., Sun-Mack, S., Young, D. F., Heck, P. W., Garber, D. P., Chen, Y., Spangenberg, D. A., Arduini, R. F., Trepte, Q. Z., Smith, W. L., et al., "Ceres edition-2 cloud property retrievals using trmm virs and terra and aqua modis datapart i: Algorithms," *IEEE Transactions on Geoscience and Remote Sensing* **49**(11), 4374–4400 (2011).

[17] Menzel, W. P., Frey, R. A., Zhang, H., Wylie, D. P., Moeller, C. C., Holz, R. E., Maddux, B., Baum, B. A., Strabala, K. I., and Gumley, L. E., "Modis global cloud-top pressure and amount estimation: Algorithm description and results," *Journal of Applied Meteorology and Climatology* **47**(4), 1175–1198 (2008).

[18] Heidinger, A. K., Evan, A. T., Foster, M. J., and Walther, A., "A naive bayesian cloud-detection scheme derived from calipso and applied within patmos-x," *Journal of Applied Meteorology and Climatology* **51**(6), 1129–1144 (2012).

[19] Walther, A. and Heidinger, A. K., "Implementation of the daytime cloud optical and microphysical properties algorithm (dcomp) in patmos-x," *Journal of Applied Meteorology and Climatology* **51**(7), 1371–1390 (2012).

[20] Schulz, J., Albert, P., Behr, H.-D., Caprion, D., Deneke, H., Dewitte, S., Dürr, B., Fuchs, P., Gratzki, A., Hechler, P., et al., "Operational climate monitoring from space: the eumetsat satellite application facility on climate monitoring (cm-saf).," *Atmospheric Chemistry & Physics* **9**(5) (2009).

[21] Finkensieper, S., Meirink, J.-F., van Zadelhoff, G.-J., Hanschmann, T., Benas, N., Stengel, M., Fuchs, P., Hollmann, R., and Werscheck, M., "Claas-2: Cm saf cloud property dataset using seviri - edition 2.," *Satellite Application Facility on Climate Monitoring* **1**(1) (2016).

[22] Stubenrauch, C., Rossow, W., Kinne, S., Ackerman, S., Cesana, G., Chepfer, H., Di Girolamo, L., Getzewich, B., Guignard, A., Heidinger, A., et al., "Assessment of global cloud datasets from satellites: Project and database initiated by the gewex radiation panel," *Bulletin of the American Meteorological Society* **94**(7), 1031–1049 (2013).

[23] Stubenrauch, C., Rossow, W., Kinne, S., Ackerman, S., Cesana, G., Chepfer, H., and Di, L., "Assessment of global cloud data sets from satellites," *A Project of the World Climate Research Programme Global Energy and Water Cycle Experiment (GEWEX) Radiation Panel* (2012).

[24] Garcia, P., Benarroch, A., and Riera, J. M., "Spatial distribution of cloud cover," *International Journal of Satellite Communications and Networking* **26**(2), 141–155 (2008).